A new unambiguous BOC(n,n) signal tracking technique

Olivier Julien, M. Elizabeth Cannon, Gerard Lachapelle, Cécile Mongrédien, Christophe Macabiau

A New Unambiguous BOC(n,n) Signal Tracking Technique*

Olivier Julien, M. Elizabeth Cannon, Gérard Lachapelle, Cécile Mongrédien
PLAN Group,
Department of Geomatics Engineering,
University of Calgary,
Canada

Christophe Macabiau
ENAC,
France

* Patent Pending

ABSTRACT
GALILEO, the major contribution of the European Union to the Global Navigation Satellite System (GNSS), will be both independent and complementary to the current GPS. It is still in its design phase, and while the signals have to be finalized, the main specifications have already been confirmed. The Binary Offset Carrier (BOC) modulation is part of the current GALILEO signal plan.
A BOC modulation multiplies a spreading code with a square wave sub-carrier that has a frequency multiple of the code rate. It creates a split spectrum with two main lobes shifted from the center frequency by the frequency of the sub-carrier. This modulated signal induces better tracking in white noise and better inherent multipath mitigation compared to the spreading code alone. However, it also makes acquisition more challenging and tracking potentially ambiguous due to its multiple peak autocorrelation function. As a result, an evaluation of its performance under different conditions and research on advanced tracking techniques are necessary to assess its robustness and advantages before final selection.
This paper focuses on a specific BOC signal: the BOC(1,1). Working on a given signal, instead of trying to find a generic solution, offers the possibility to fully exploit this signal's characteristics to find a more relevant way to improve its performance and cancel its bias threat. A new innovative tracking technique dedicated to BOC(n,n) signals has therefore been developed using a synthesized local correlation function. It completely removes the side-peak threat and allows clean acquisition and tracking of any BOC(n,n) signal while keeping the same sharp correlation main peak. Consequently, it does not need to check if tracking is done on the main peak. It also offers a good resistance to long-delay multipath. The particular case of BOC(1,1) is taken as an example throughout the paper due to the strong probability that it will be used by the L1 GALILEO civil signal. Both acquisition and tracking are studied and compared with the standard tracking algorithm, first theoretically and then using simulations.

INTRODUCTION
In the new generation of Global Navigation Satellite Systems (GNSSs), special attention has been made to have efficient and spectrally relevant signals. GALILEO and GPS will share two central frequencies and will both send several signals on the same carriers. Consequently, new signal modulations had to be studied to minimize inter- and intra-system interference. One modulation emerged due to its split spectrum that spectrally isolates the signal from the currently used Bi-Phased Shift Keying (BPSK) modulation [Godet et al., 2002; Betz, 2002]. This new modulation is known as Binary Offset Carrier (BOC). It multiplies a spreading code with a square wave sub-carrier that has a frequency multiple of the spreading code frequency. This creates a symmetric split spectrum with two main lobes shifted from the carrier frequency by the value of the sub-carrier frequency. The properties of the BOC signals are dependent on the spreading code chip rate, the sub-carrier frequency, and the sub-carrier phasing within one PRN code chip. The common notation for BOC-modulated signals in the GNSS field is BOC(f_c,f_s) where f_c represents the code chip rate, and f_s is the frequency of the sub-carrier. Both f_c and f_s are usually noted as a multiple of the reference frequency 1.023 MHz.
A summary of all the basic properties and improvements brought by BOC signals compared to BPSK signals is given by Betz (2002). Among others, it is worth noting that for the same chip rate, BOC signals have a lower inherent tracking noise, and better multipath and narrow-band interference

mitigation. However, the presence of the sub-carrier introduces several peaks in the range [-1, +1] chip in BOC autocorrelation. Figure 1 shows the autocorrelation of a BPSK signal with a 1.023 MHz spreading code rate and a sine-phased BOC(1,1) with the same spreading code. As observed, BOC autocorrelation presents secondary peaks. The presence of these secondary peaks may cause a serious problem if the receiver locks onto a side peak instead of the main peak. A significant bias of approximately 150 m would then be present in the range measurements, which is unacceptable for navigation applications.

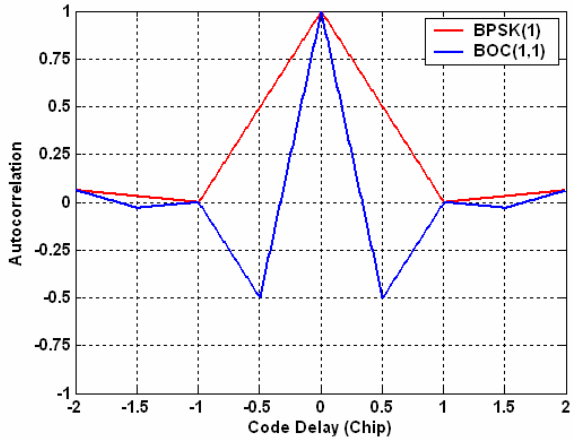

Figure 1 – Normalized Autocorrelation for BPSK(1) and sine phased BOC(1,1)

Several methods have been proposed to track BOC signals without suffering from any potential tracking bias. Fine and Wilson (1999), Lin et al. (2003), Martin et al. (2003) and Ward (2004) are a few examples. They treat the problem of the BOC tracking ambiguity in a broad sense, trying to find a solution that could be applied to any BOC(n,m) signal. This paper differs from this approach by studying an unambiguous tracking specific to BOC(1,1) signals. The choice of the BOC(1,1) is due the significant possibility that it will be used for the GALILEO civil signal on the E2-L1-E1 band. Moreover, there are also discussions to introduce it as a candidate for the GPSIII civil signal on the L1 band [Gibbon, 2004]. This makes the BOC(1,1) signal particularly interesting to study. The research on a single type of BOC signal put forward the desire to exploit fully the particularities of this signal to try to find potentially improved solutions than the ones already known. However, because the structure of a BOC signal depends upon the relation between the spreading code frequency and the sub-carrier frequency, a solution for BOC(1,1) signals can be directly extended to any BOC(n,n) signals. The new unambiguous tracking method introduced herein uses the particular correlation between a BOC(n,n) signal and its spreading code (without the sub-carrier) to synthesize a single-peak correlation function. It therefore avoids constant checking to ensure that the main peak is being tracked, as necessary on a standard BOC tracking technique. It is important to mention that the new technique presented herein could be extended to other BOC signals, however it may not be optimal for other BOC modulations due to its dedication to BOC(n,n) characteristics. For the sake of simplicity, only BOC(1,1) signals will be studied.

The first part of this paper details the BOC(1,1) tracking ambiguity problem to underline the motivation for this research. A new unambiguous synthesized correlation function and its generation are then presented. A new Early-Minus-Late Power (EMLP) discriminator, adapted to the new correlation function, is investigated in the third part and its tracking technique performance is given through extensive simulations thereafter. The inherent multipath mitigation performance of the new tracking technique is then shown. Finally, an unambiguous acquisition scheme using the proposed synthesized correlation is introduced.

BOC(1,1) RANGING AMBIGUITY ISSUE

Although it is well-known that BOC signals have a tracking ambiguity issue, the understanding and quantification of the threat is a prerequisite to ensure the relevance of the research. Two main sources can lead to a ranging ambiguity when using BOC modulation for ranging:

- A short loss of lock (due to a low C/N_0 for instance) followed by the lock, after a drift of the code tracking, on a secondary peak (an increase of the C/No shortly after the loss of lock)
- An incorrect acquisition that would acquire on the secondary peak of the autocorrelation function and be followed by ambiguous tracking.

As this research is dedicated to the unambiguous tracking of BOC(n,n) signals, the two issues mentioned above that could lead to a range bias, are specifically studied hereafter in the context of the BOC(1,1) signal.

Tracking Ambiguity

The autocorrelation function of the BOC(1,1) signal with sine phasing, R_{BOC} , plotted in Figure 1, can be written as follows:

$$R_{BOC}(\tau) = tri_0\left(\frac{\tau}{1}\right) - \frac{1}{2}tri_{\frac{1}{2}}\left(\frac{\tau}{1}\right) - \frac{1}{2}tri_{-\frac{1}{2}}\left(\frac{\tau}{1}\right) \qquad (1)$$

where $tri_\alpha\left(\frac{x}{y}\right)$ is the value in x of a triangular function centred in α with a base width of y and a peak magnitude of 1; τ is the code delay in chips.

Assuming that the Delay Lock Loop (DLL) uses an EMLP discriminator, the theoretical expression of the discriminator output is:

$$V_{EMLP}^{BOC}(\varepsilon_\tau) = \left[\left[IE_{BOC}{}^2 + QE_{BOC}{}^2\right] - \left[IL_{BOC}{}^2 + QL_{BOC}{}^2\right]\right] \qquad (2)$$

Assuming the code tracking error ε_τ is smaller than half the Early-Late spacing C_s, and that C_s is smaller than one chip, the EMLP discriminator expression in the central region is given by:

$$V_{EMLP}^{BOC}(\varepsilon_\tau) = \frac{A^2}{4}[18\varepsilon_\tau C_s - 12\varepsilon_\tau] \quad (3)$$

$$\text{for } -\frac{C_s}{2} \le \varepsilon_\tau \le \frac{C_s}{2}$$

where A is the amplitude of the incoming signal.

Normalizing the discriminator is mandatory in order to eliminate the dependency of that signal upon the received signal power. The normalization typically used for an EMLP discriminator is:

$$NORM = \left[(IE_{BOC} + IL_{BOC})^2 + (QE_{BOC} + QL_{BOC})^2\right] \quad (4)$$

As a consequence, the normalized standard BOC(1,1) EMLP discriminator can be expressed as:

$$V_{NORM}^{BOC}(\varepsilon_\tau) = \frac{(2-3C_s)^2 V_{EMLP}^{BOC}(\varepsilon_\tau)}{(18C_s - 12)NORM} \quad (5)$$

$$\text{for } -\frac{C_s}{2} \le \varepsilon_\tau \le \frac{C_s}{2}$$

Figure 2 shows the normalized EMLP discriminator output for an early-late spacing of 0.2 chips using a 6 MHz double-sided front-end filter. The stability domain is clearly identified around the zero code delay in the [-0.33; 0.33] chip region. However, two other stable lock points can be identified around a code delay of ±0.55 chips. These two false lock points represent the threat of a tracking bias. A code tracking error greater than 0.33 chips would lead to a biased lock.

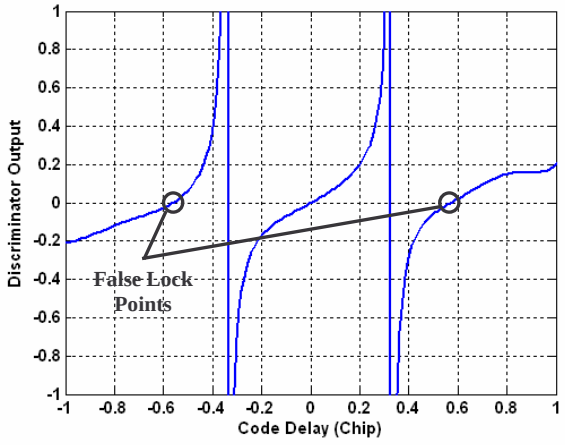

Figure 2 – Standard Normalized BOC(1,1) EMLP Discriminator for an Early-Late Spacing of 0.2 Chips (6 MHz Double-Sided Front-End Filter)

It is interesting to note as well that the two false lock points are not situated exactly at the same code delay as the secondary peak (0.5 chips), but slightly beside due to the different slopes constituting the secondary peaks.

It is now clear that high noise, or incorrect acquisition that would output the code delay of a secondary peak, would lead to biased tracking. To quantify this threat, the probability of missed acquisition has to be studied.

Acquisition Ambiguity

The BOC(1,1) has an autocorrelation function that has secondary peaks with a magnitude of 0.5 relatively to its main peak, as seen in Figure 1. This will of course have an impact on the acquisition performance, as unlike the cross-correlation peaks, this relative magnitude will remain constant whatever the C/N_0 value. In order to visualize the probability of acquiring on the secondary peak, an analysis based upon the theory described by Bastide et al. (2002) has been followed. This method, valid for signals spread by a standard pseudo-random code can be fully used when a sub-carrier modulates the code because the cross-correlation peaks of the BOC signals have the same magnitude as those of the spreading code. In order to set the acquisition thresholds, a probability of false alarm (P_{fa}) of 10^{-3} has been chosen and an interfering signal with a C/N_0 of 45 dB-Hz has been assumed. The computations assumed the same correlation isolation for the spreading code as that of the GPS C/A-code correlation function. Figure 3 shows the probability of detection of the main and secondary peaks of the BOC(1,1) signals assuming that neither Doppler nor code delay error is present, for a coherent integration time of 1 ms and for 15, 40 and 60 non-coherent summations.

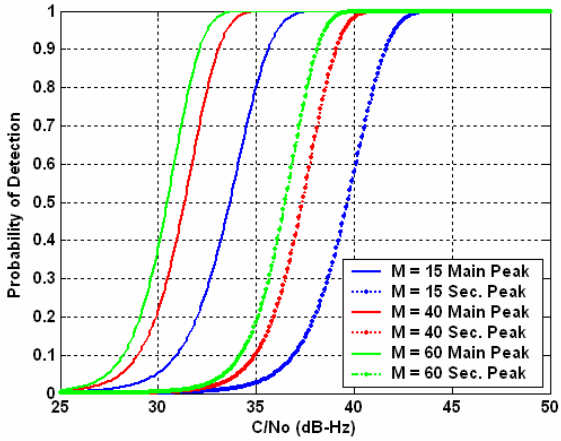

Figure 3 – Probability of Detection of the Main and Secondary Peaks of the BOC(1,1) Signals for 15, 40 and 60 Non-Coherent Summations and Coherent Integration Time of 1 ms

As expected, the probabilities of detection of the secondary peaks are offset from the ones of the main peak by 6 dB, which is the difference in the correlation power between the two peaks. It can be observed from Figure 3 that when the C/N_0 reaches 35 to 40 dB-Hz, the secondary peaks can be considered as real threats for acquisition due to its

non-negligible probability of detection. It has to be underlined that the 6 dB difference between the curves corresponding to main and secondary peaks is not the worst case. Indeed, the search cells could fall slightly on the side of the main peak and so have a lower probability of detection that the one indicated in Figure 3 for a given C/N_0.

In order to further emphasize the problem that the combination of wrong acquisition followed by ambiguous tracking can provide, a simulation was set up. Using the normalized EMLP discriminator already described, an initial code delay value of 0.5 chips was fed to the tracking loops (assuming correct Doppler). The BOC(1,1) signal was simulated using the GPS C/A-code as its spreading code. The C/N_0 was chosen to be 40 dB-Hz, the coherent integration time was 1 ms and the DLL loop filter was set to 2 Hz. Figure 4 shows the results of this test. The DLL clearly locks onto the secondary peak and remains approximately 0.55 chips away from the true delay, confirming the stability of the lock point.

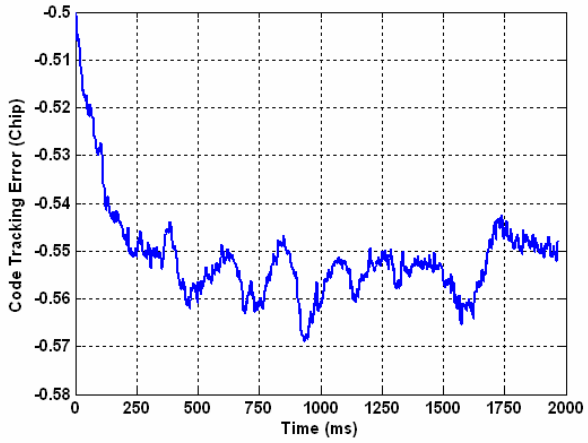

Figure 4 – Example of Biased BOC(1,1) Tracking on False Peak with an Initial Code Delay Error of -0.5 Chips (2 Hz DLL)

Now that the threat created by the BOC(1,1) multi-peak autocorrelation function has been highlighted, it is of great importance to try to find a relevant way to get ride of this problem. A new method, using an unambiguous synthesized correlation function, is therefore presented.

A NEW UNAMBIGUOUS BOC(1,1) SYNTHESIZED CORRELATION FUNCTION

One intuitive technique to get an unambiguous discrimination function comes when studying the two following correlation functions:

- Autocorrelation of BOC(1,1) signals, R_{BOC}, whose autocorrelation function is given in equation (1), considering an infinite front end filter,
- Cross-correlation $R_{BOC/PRN}$ of a BOC(1,1) signal with its spreading code PRN (without the sub-carrier), which can be expressed as (see Appendix A):

$$R_{BOC/PRN}(\tau) = \frac{1}{2}\left(tri_{-\frac{1}{2}}\left(\frac{\tau}{1}\right) - tri_{\frac{1}{2}}\left(\frac{\tau}{1}\right)\right) \qquad (6)$$

As shown in equations (1) and (6), the side-peaks of the BOC(1,1) autocorrelation have the same absolute magnitude and the same location as the two peaks of the BOC(1,1)/PRN cross-correlation function. In order to take advantage of this, a new synthesized correlation function can be obtained by differencing the squared correlation points of these two functions. Figure 5 shows the two squared correlation functions using a 6 MHz double-sided filter and the resulting synthesized correlation function. As seen in Figure 5, it succeeds in cancelling almost totally the two side-peaks of the BOC(1,1) autocorrelation function. Moreover, its main peak keeps the same sharpness which is of great importance when considering tracking performance. Two negative side-lobes appear next to the main peak (around ±0.35 chips) due to unmatched slopes between the two correlation functions initially considered. They bring no threat as potential lock points as they point downwards. The correlation values obtained after 0.5 chips are very close to zero.

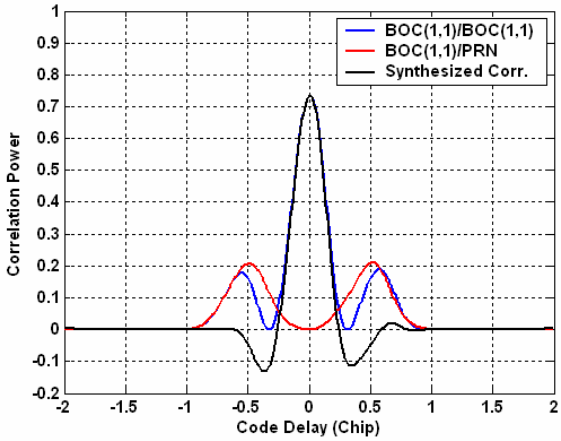

Figure 5 – Normalized Squared BOC(1,1) Autocorrelation , BOC(1,1)/PRN Correlation, and Synthesized Correlation Obtained by Differencing Both (6 MHz Double-Sided Front-End Filter)

The expression for the synthesized correlation function in the case of an infinite front-end bandwidth is obtained by subtracting the square of equations (1) and (6):

$$R_{SYN}(\tau) = \left(tri_0\left(\frac{\tau}{1}\right)\right)^2 - tri_0\left(\frac{\tau}{1}\right) \times \left[tri_{\frac{1}{2}}\left(\frac{\tau}{1}\right) + tri_{-\frac{1}{2}}\left(\frac{\tau}{1}\right)\right] \qquad (7)$$

PROPOSED BOC(1,1) DLL DISCRIMINATOR DERIVATION

Due to the symmetry and shape of the new synthesized correlation function, it is intuitive to consider code tracking discriminators close to the ones already used for the standard BOC(1,1)

tracking. Consequently, an EMLP discriminator is proposed hereafter. Before calculating its complete formulation, ideal expressions of the BOC(1,1) autocorrelation and BOC(1,1)/PRN correlation functions should be given in the central region. For this purpose, assuming that the code tracking error, ε_τ, is smaller than half the spacing C_s between the early and late correlators, the discrimination function, in the absence of filtering and noise, can then be rewritten as follows using equation (1):

$$R_{BOC}(\tau) = 1 - 3|\tau| \text{ for } |\tau| \le \frac{1}{2} \quad (8)$$

Similarly, $R_{BOC/PRN}(\tau)$ can be expressed as:

$$R_{BOC/PRN}(\tau) = -\tau \quad \text{for } |\tau| \le \frac{1}{2} \text{ (sine phasing)} \quad (9)$$

An EMLP discriminator adapted to the new correlation function is studied hereafter.

Assuming that $V_{EMLP}^{BOC/PRN}$ is the output of the EMLP discriminator, it follows that:

$$V_{EMLP}^{BOC/PRN}(\varepsilon_\tau) = \left[\left[IE_{BOC}{}^2 + QE_{BOC}{}^2\right] - \left[IL_{BOC}{}^2 + QL_{BOC}{}^2\right]\right] - \left[\left[IE_{BOC/PRN}{}^2 + QE_{BOC/PRN}{}^2\right] - \left[IL_{BOC/PRN}{}^2 + QL_{BOC/PRN}{}^2\right]\right] \quad (10)$$

The EMLP discrimination function can then be expressed as:

$$V_{EMLP}^{BOC/PRN}(\varepsilon_\tau) = \frac{A^2}{4}\left[R_{BOC}\left(\varepsilon_\tau + \frac{C_S}{2}\right)^2 - R_{BOC}\left(\varepsilon_\tau - \frac{C_S}{2}\right)^2\right] - \frac{A^2}{4}\left[R_{BOC,PRN}\left(\varepsilon_\tau + \frac{C_S}{2}\right)^2 - R_{BOC,PRN}\left(\varepsilon_\tau - \frac{C_S}{2}\right)^2\right] \quad (11)$$

So, assuming $-\frac{C_s}{2} \le \varepsilon_\tau \le \frac{C_s}{2}$, the final expression of the EMLP discriminator is given by:

$$V_{EMLP}^{BOC/PRN}(\varepsilon_\tau) = \frac{A^2}{4}\left[18\varepsilon_\tau C_s - 12\varepsilon_\tau\right] - \frac{A^2}{4}\left[2\varepsilon_\tau C_s\right] \quad (12)$$

$$\text{for } -\frac{C_s}{2} \le \varepsilon_\tau \le \frac{C_s}{2}$$

It is interesting to note that an EMLP discriminator that would use a pure BOC(1,1) local signal would only vary as the first component of that expression as seen in equation (3). The slope of the pure BOC(1,1) EMLP discriminator is $18C_S - 12$, which has an absolute value lower than the slope of the new proposed discriminator $16C_S - 12$.

As already discussed, normalizing the discriminator is essential to estimate the amplitude term in the discriminator. However, it is also important to make sure that this normalization does not limit the stability domain of the discriminator. It is also of critical importance to have a normalized discriminator with a 'correct' response for a code tracking error as large as possible.

Three normalizations of the EMLP discriminator were studied. The first one is based on the same method as used by the BOC(1,1) EMLP discriminator, i.e.

$$NORM1 = \left[\left(IE_{BOC} + IL_{BOC}\right)^2 + \left(QE_{BOC} + QL_{BOC}\right)^2\right] + \left[\left(IE_{BOC/PRN} + IL_{BOC/PRN}\right)^2 + \left(QE_{BOC/PRN} + QL_{BOC/PRN}\right)^2\right] \quad (13)$$

It leads to the following output expression:

$$V_{NORM1}^{BOC/PRN}(\varepsilon_\tau) = \frac{(2 - 3C_S)^2 V_{EMLP}^{BOC/PRN}}{(16C_S - 12)NORM1} \quad (14)$$

$$\text{for } -\frac{C_s}{2} \le \varepsilon_\tau \le \frac{C_s}{2}$$

The second expression uses the same normalization as the standard BOC(1,1), namely:

$$NORM2 = \left[\left(IE_{BOC} + IL_{BOC}\right)^2 + \left(QE_{BOC} + QL_{BOC}\right)^2\right] \quad (15)$$

which gives the following normalized output:

$$V_{NORM2}^{BOC/PRN}(\varepsilon_\tau) = \frac{(2 - 3C_S)^2 V_{EMLP}^{BOC/PRN}}{(16C_S - 12)NORM2} \quad (16)$$

$$\text{for } -\frac{C_s}{2} \le \varepsilon_\tau \le \frac{C_s}{2}$$

Finally, the last normalization studied was a slightly modified version of the first one, but it takes into account the anti-symmetrical property of the BOC(1,1)/PRN correlation function:

$$NORM3 = \left[\left(IE_{BOC} + IL_{BOC}\right)^2 + \left(QE_{BOC} + QL_{BOC}\right)^2\right] + \left[\left(IE_{BOC/PRN} - IL_{BOC/PRN}\right)^2 + \left(QE_{BOC/PRN} - QL_{BOC/PRN}\right)^2\right] \quad (17)$$

The normalized discriminator output then becomes:

$$V_{NORM3}^{BOC/PRN}(\varepsilon_\tau) = \frac{\left(4 - 12C_s + 10C_s{}^2\right)V_{EMLP}^{BOC/PRN}}{(16C_S - 12)NORM3} \quad (18)$$

$$\text{for } -\frac{C_s}{2} \le \varepsilon_\tau \le \frac{C_s}{2}$$

Figure 6 shows the output of the three normalized EMLP discriminators described as well as the output of the standard normalized BOC(1,1) discriminators for an early-late spacing of 0.2 chips. It is very important to note that unlike the standard BOC(1,1) discriminator that has a false lock point, there is no such potential problem for the three proposed new discriminators. This confirms that the new synthesized correlation function cannot lead to an ambiguous measurement. However, the three proposed normalizations will lead to different tracking performances due to their impact on the discriminator output shape. The first normalization seems to have weaker performance compared to the two others due to its quick return to 0 when the code tracking error becomes greater than 0.2 chips. The two other normalizations, $NORM2$ and $NORM3$, have similar responses and have stability areas slightly greater than the standard BOC(1,1) EMLP discriminator: [-0.38; 0.38] chips compared to [-0.33; 0.33] chips. This is very important, as it means that the new synthesized EMLP discriminator using one of these two normalizations will have a slightly larger

resistance to tracking errors than pure BOC(1,1) tracking.

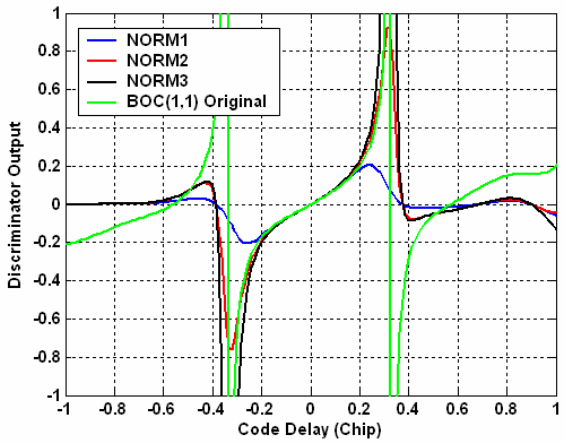

Figure 6 –Synthesized EMLP Discriminator Output for the Three Proposed Normalizations, and for the Original Normalized BOC(1,1) EMLP Discriminator for an Early-Late Spacing of 0.2 Chips (6 MHz Double-Sided Front-End Filter)

Plotting the same discriminators with different early-late spacings leads to the same conclusions, the stability domain just changes as a function of C_s. In order to avoid losses of lock due to large discriminator output around the limits of the stability domain for $NORM2$ and $NORM3$, a cut-off value dependent upon C_s should be used.

The study of their relative performance in the presence of Gaussian noise will be studied using simulations because the theoretical analysis of the tracking loops in such conditions is fastidious and difficult when considering normalization. The results of these simulations are shown in the following section.

Note also that a dot-product type of discriminator has been analyzed (also unambiguous), but due to the space limitation, it will not be investigated in this paper.

OBSERVED BOC(1,1) TRACKING PERFORMANCE WITH THE PROPOSED TECHNIQUE

The Phase Lock Loop (PLL) needs to have the correct phase information on both the in-phase and quadra-phase channels in order to consistently estimate the phase offset. This cannot be achieved by using the values of the synthesized correlators because of their squaring that corrupts the phase information. As a consequence, the PLL is run using the prompt values of the standard BOC(1,1) correlators. As a result, the PLL is exactly the same as in classical BOC(1,1) tracking.

The first test undertaken was meant to confirm that the new discriminator avoids any false lock point. For this test, as described previously, three different normalized EMLP discriminators were compared. The first one uses the standard normalized BOC(1,1) EMLP discriminator. The two others use the synthesized EMLP discriminators with two different normalizations: $NORM2$ and $NORM3$. A PLL-aided DLL is used. As already discussed, a cut-off value was set for the three discriminators' outputs. It was decided that by using a 0.2 chip early-late spacing, the discriminator output would be set to 0.4 chips whenever the actual absolute value of the output was greater than 0.4 chips. The front-end filter has a double-sided bandwidth of 6 MHz. The DLL and PLL loop bandwidths were set to 1 and 10 Hz respectively. The integration time was chosen to be 1 ms and the initial code delay was set to 0.5 chips, assuming an acquisition on the side peak. The C/N_0 is 40 dB-Hz. Figure 7 shows the results of this test.

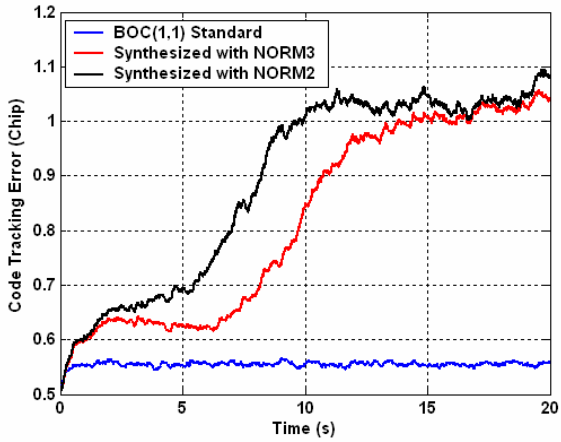

Figure 7 – Tracking Response of the Three Methods Considered With an Initial Code Delay of 0.5 Chips (10 Hz PLL, 1 Hz DLL, PLL-aided DLL, 1 ms Integration Time)

Figure 7 shows that unlike the BOC(1,1) standard discriminator, the two others do not make the DLL lock on any offset stable point, confirming the results shown in Figure 6. The use of the same PLL as in standard BOC(1,1) tracking could have raised a concern as the PLL aiding uses standard BOC(1,1) prompt correlation values. One could have imagined that it would have limited the drift from the biased initial code delay, following the estimation coming from the PLL. Figure 7 shows that it is not the case.

An easy way to detect the loss of lock, however, is to analyze the output of the prompt correlators of the new method. As there are no false lock points once outside the stability domain, and that the synthesized correlation value after 0.5 chips is very close to zero, the correlators output will average to zero. Figure 8 underlines this point by showing the in-phase prompt correlators' outputs for the different strategies. The blue points represent the in-phase output of the BOC(1,1) standard technique, so squaring has not been applied, while for the red and black curves, the in-phase prompt correlators output is the one modeled by equation (10) (but in the prompt case).

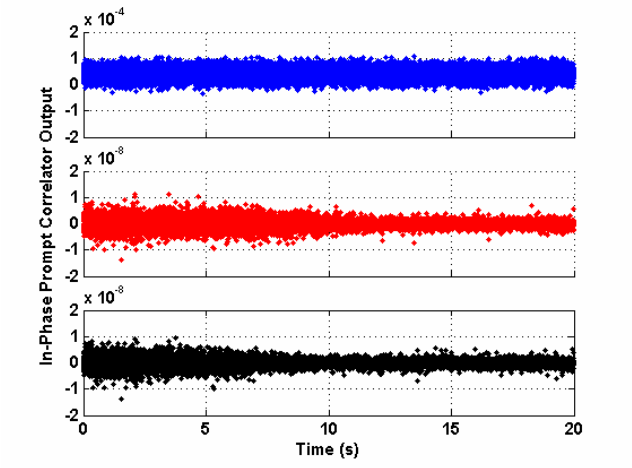

Figure 8 - In-Phase Prompt Correlators' Output of the Different Strategies (Blue: Standard BOC(1,1); Red: Synthesized Using $NORM3$; Synthesized Using $NORM2$) (10 Hz PLL, 1 Hz DLL, PLL-aided DLL, 1 ms Integration Time)

Now that the unambiguous new tracking technique has been confirmed, an extensive series of tests were realized to compare the noise of the two candidate normalizations. Indeed, the noise effect on the two proposed normalized EMLP discriminators still has to be investigated. The tests were run with the same settings as described previously. This time however, the initial code delay was set to 0.1 chips in order to observe the convergence toward zero, a strong clue for correct tracking, as well as to study the code tracking noise when convergence is achieved. The simulations were run over 20 seconds of simulated data. The exact same tracking parameters as the ones used to obtain Figure 7 were chosen. Figure 9 shows the results of this simulation for a signal with a C/N_0 of 40 dB-Hz.

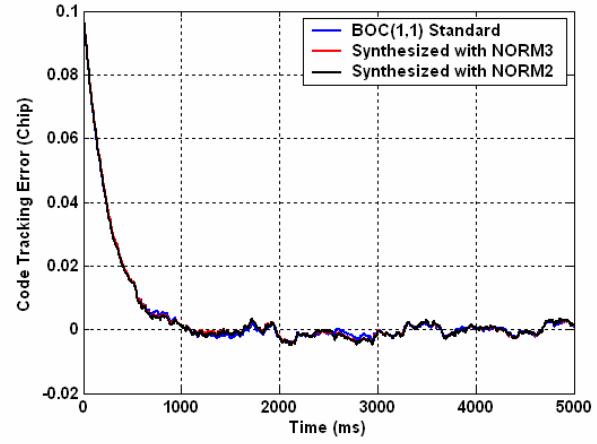

Figure 9 – Code Tracking Error for the Three Considered Tracking Techniques for a 5 Second Test for a C/N_0 = 40 dB-Hz (10 Hz PLL, 1 Hz DLL, PLL-aided DLL, 1 ms Integration Time)

The convergence period in Figure 9 takes approximately 1 second. The standard deviation of the code tracking error is computed for all the output obtained after two seconds of data processed in order to make sure that the values used are after the convergence. In order to have a reliable analysis, tests were done independently on two different software receivers: one developed by ENAC, Toulouse, France, and one developed by the University of Calgary, Canada. Figure 10 summarizes the results obtained during the simulation campaign. For all the cases considered, convergence was obtained.

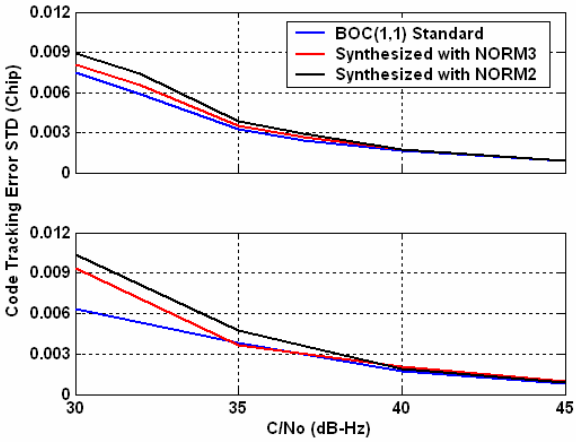

Figure 10 - Standard Deviation of the Code Tracking Errors for the Three Methods Considered (10Hz PLL, 1Hz DLL, PLL-aided DLL, 1ms Integration Time) for UofC (Top) and ENAC (Bottom) Simulators

Figure 10 shows very consistent results, which confirm the correctness of the implementation (although a doubt remains for 30 dB-Hz). Comparing the two new normalized discriminators, the one using $NORM3$ always outperforms the one using $NORM2$. Although the difference is very small for high C/N_0, it increases as the signal strength decreases. This is essentially due to the fact that the third normalization uses the same components as the synthesized not-normalized EMLP discriminator. Consequently, $NORM3$ should be the normalization selected when using the new synthesized EMLP discriminator.

However, its noise mitigation performance is still slightly worse than for code tracking using the standard normalized BOC(1,1) discriminator. The main reason can be explained by viewing the new synthesized discriminator as the difference of two EMLP discriminators: one associated with the pure BOC(1,1) autocorrelation, and the other one with the BOC/PRN correlation. This linear combination brings extra noise that is partially cancelled by the correlation of both pairs' noise values. However, there is still extra noise entering the tracking loops. The ratio between the code tracking error standard deviations is between 1.07 and 1.22 (excluding 30 dB-Hz results) according to the tests considered,

which is very small. When looking at Figure 10, this represents a loss in C/N_0 of less than 1 dB.
Because the PLL used in each case is exactly the same, the phase tracking errors are equivalent between the different methods.
Another important performance parameter when studying a tracking technique is its inherent resistance to multipath which is investigated in the next section.

BOC(1,1) MULTIPATH MITIGATION PERFORMANCE USING THE PROPOSED TRACKING DISCRIMINATOR

As already mentioned, the new synthesized correlation function has a support function smaller than that of the BOC(1,1) autocorrelation function. In the ideal case of infinite bandwidth, it has non-zero values only within ± 0.5 chips. However, due to the use of a non-linear combination of correlators' output to form the discriminators, it does not imply that the impact of long delay multipath is cancelled. Figure 11 shows the multipath envelope of the standard and synthesized EMLP discriminators for a received multipath of half the direct signal power and an early-late spacing of 0.2 chips. The front end filter used has a 6 MHz double-sided bandwidth. The multipath envelope of the new unambiguous technique has the same shape as the one of the traditional BOC(1,1) tracking method. However, they have two main differences: (1) the first lobe of the new method is slightly wider for multipath delays between 0.25 and 0.55 chips; (2) the second lobe for the new tracking method is narrower, implying a better multipath rejection for long delay multipath. It has to be noticed that the choices of the front-end filter bandwidth and of the early-late spacing have an impact in the magnitude of the difference between the two methods. However, it gives the same general shape. This result is still very interesting, as the new synthesized method offers a good resistance to long delay multipath while giving reliable measurements. It is also important to underline two important drawbacks of the traditional BOC(1,1) tracking technique when multipath are present. First, the multipath envelope plotted in Figure 11 is not realistic, as it assumes a correct tracking which might not be occurring. Secondly, it has to be noticed that using the traditional method, it is possible that a strong multipath creates an interfering correlation peak that is higher or as high as the secondary peak of the BOC(1,1) autocorrelation function. In such a case, if the receiver is tracking the secondary peak, this can dangerously mislead the receiver.
As already seen, the stability domain of the proposed new discriminator is slightly greater than the one associated with the standard EMLP BOC(1,1) discriminator. Its tracking performance is quasi-equivalent to standard BOC(1,1) tracking. Finally, it has a better inherent mitigation of long-delay multipath. However, if the initial tracking error is greater than approximately 0.35 chips the discriminator will not be able to converge toward zero code delay, and the loop will lose lock. Note that the behavior of pure BOC(1,1) tracking in that case would be to slide to a false lock point as presented in the first section. This means that in order to make sure that the receiver using the new tracking technique succeeds in tracking the incoming signal it has to acquire the signal relatively close to the main peak. As already seen, this may be a problem when using a conventional acquisition technique based on a search of the maximum energy using the autocorrelation power due to the presence of the side peaks. For this reason, an investigation of an acquisition technique using the synthesized correlation function is done hereafter.

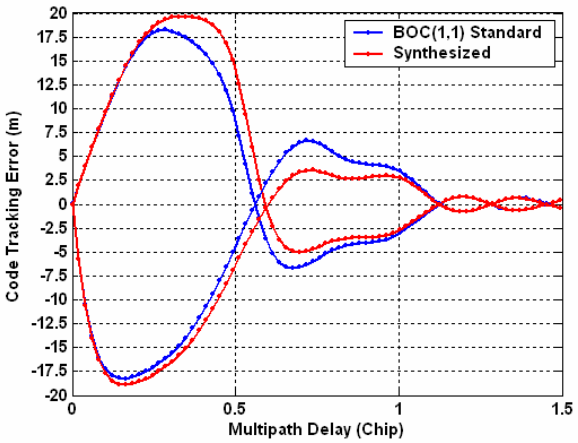

Figure 11 – Multipath Envelopes for the Standard BOC(1,1) and new Synthesized EMLP Discriminators for a Single Multipath with Half the Power of the Direct Signal and an Early-Late Spacing of 0.2 Chips (6 MHz Double-Sided Front-End Filter)

BOC(1,1) ACQUISITION USING THE SYNTHESIZED CORRELATION FUNCTION

Figure 12 illustrates the receiver acquisition structure.

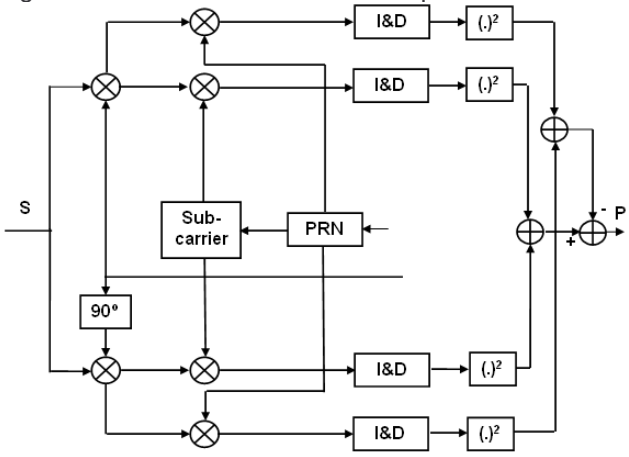

Figure 12 – Synopsis of the New Acquisition Structure

Assuming that M is the number of non-coherent summations, the signal power at the output of the synthesized correlation is given by:

$$P = \sum_{k=1}^{M} \left(\left(I_{BOC_k}^2 + Q_{BOC_k}^2 \right) - \left(I_{BOC/PRN_k}^2 + Q_{BOC/PRN_k}^2 \right) \right) \quad (19)$$

Since the noise power at each correlator's output is the same, it is possible to have the following acquisition criterion:

$$\frac{P}{\sigma_n^2} = \sum_{i=1}^{M} \left[\begin{array}{l} \left(\sqrt{\frac{CT_p}{N_0}} R_{BOC}(\varepsilon_\tau) \frac{\sin(\pi f_D T_p)}{\pi f_D T_p} \cos(\varepsilon_\theta) + n_{IBOC} \right)^2 \\ + \left(\sqrt{\frac{CT_p}{N_0}} R_{BOC}(\varepsilon_\tau) \frac{\sin(\pi f_D T_p)}{\pi f_D T_p} \sin(\varepsilon_\theta) + n_{QBOC} \right)^2 \\ - \left(\sqrt{\frac{CT_p}{N_0}} R_{BOC/PRN}(\varepsilon_\tau) \frac{\sin(\pi f_D T_p)}{\pi f_D T_p} \cos(\varepsilon_\theta) + n_{IBOC/PRN} \right)^2 \\ - \left(\sqrt{\frac{CT_p}{N_0}} R_{BOC/PRN}(\varepsilon_\tau) \frac{\sin(\pi f_D T_p)}{\pi f_D T_p} \sin(\varepsilon_\theta) + n_{QBOC/PRN} \right)^2 \end{array} \right] \quad (20)$$

where σ_n^2 is the variance of the correlator's output noise with power $\frac{N_0}{4T_p}$; T_p is the coherent integration time; C is the signal power at the output of the receiver antenna; n_{IBOC}, n_{QBOC}, $n_{IBOC/PRN}$ and $n_{IBOC/PRN}$ are centred Gaussian noise with a unity variance; ε_θ is the phase error; and f_D is the frequency error.

The acquisition criterion can be seen as the difference between two non-central Chi-square distributions. Consequently, the acquisition criterion can be defined as:

$$T_{new} = \frac{P}{\sigma_n^2} = T_{BOC} - T_{BOC/PRN} \quad (21)$$

where

$$T_{BOC} = \sum_{k=1}^{M} \left(\begin{array}{l} \left(\sqrt{\frac{CT_p}{N_0}} R_{BOC}(\varepsilon_\tau) \frac{\sin(\pi f_D T_p)}{\pi f_D T_p} \cos(\varepsilon_\theta) + n_{IBOC} \right)^2 \\ + \left(\sqrt{\frac{CT_p}{N_0}} R_{BOC}(\varepsilon_\tau) \frac{\sin(\pi f_D T_p)}{\pi f_D T_p} \sin(\varepsilon_\theta) + n_{QBOC} \right)^2 \end{array} \right) \quad (22)$$

and

$$T_{BOC/PRN} = \sum_{k=1}^{M} \left(\left(\begin{array}{l} \left(\sqrt{\frac{CT_p}{N_0}} R_{BOC,PRN}(\varepsilon_\tau) \frac{\sin(\pi f_D T_p)}{\pi f_D T_p} \cos(\varepsilon_\theta) + n_{IBOC/PRN} \right)^2 \\ + \left(\sqrt{\frac{CT_p}{N_0}} R_{BOC,PRN}(\varepsilon_\tau) \frac{\sin(\pi f_D T_p)}{\pi f_D T_p} \sin(\varepsilon_\theta) + n_{QBOC/PRN} \right)^2 \end{array} \right) \right) \quad (23)$$

Since the acquisition criterion is the difference between two Chi-square distributions, its expected value can be expressed as:

$$\langle T_{new} \rangle = \langle T_{BOC} \rangle - \langle T_{BOC/PRN} \rangle \quad (24)$$

As shown in Appendix A, the two distributions T_{BOC} and $T_{BOC/PRN}$ can be assumed as independent when no front-end filter was used. Empirically, this covariance has been determined to be very low when using a front-end filter, so that:

$$\sigma_{T_{new}}^2 = \sigma_{T_{BOC}}^2 + \sigma_{T_{BOC/PRN}}^2 \quad (25)$$

From equations (24) and (25), it is possible to compare the mean and variance of the new acquisition criterion with the values of the standard acquisition criterion (symbolized by T_{BOC}). For this purpose, two figures of merit have been defined: the ratio of the means ($FOM1$), and the ratio of the variances ($FOM2$). These two figures of merit can be expressed using equations (22- 25) as:

$$FOM1 = \frac{\frac{CT_p}{N_0} \left((R_{BOC}(\varepsilon_\tau))^2 - (R_{BOC,PRN}(\varepsilon_\tau))^2 \right) \left(\frac{\sin(\pi f_D T_p)}{\pi f_D T_p} \right)^2}{\frac{CT_p}{N_0} (R_{BOC}(\varepsilon_\tau))^2 \left(\frac{\sin(\pi f_D T_p)}{\pi f_D T_p} \right)^2 + 2} \quad (26)$$

and,

$$FOM2 = \frac{4\frac{CT_p}{N_0} \left((R_{BOC}(\varepsilon_\tau))^2 + (R_{BOC,PRN}(\varepsilon_\tau))^2 \right) \left(\frac{\sin(\pi f_D T_p)}{\pi f_D T_p} \right)^2 + 2}{\frac{CT_p}{N_0} (R_{BOC}(\varepsilon_\tau))^2 \left(\frac{\sin(\pi f_D T_p)}{\pi f_D T_p} \right)^2 + 1} \quad (27)$$

From equations (26) and (27), it can be seen that both figures of merit favour the standard acquisition criterion. Indeed, the ratio of the means will always be smaller than 1, meaning that $\langle T_{new} \rangle$ will always be smaller than $\langle T_{BOC} \rangle$ when the same acquisition parameters are used. Similarly, $FOM2$ will always be greater than 1, meaning that $\sigma_{T_{new}}^2$ will always be larger than $\sigma_{T_{BOC}}^2$. Due to the relatively small value of $(R_{BOC,PRN}(\varepsilon_\tau))^2$ compared to $(R_{BOC}(\varepsilon_\tau))^2$ around $\varepsilon_\tau = 0$, its impact on the acquisition performance will be small.

It is interesting to note that the number of non-coherent summations has no impact on the two figures of merit. This means that the difference between the two criteria cannot be bridged using a large number of non-coherent summations. Equations (26) and (27) also show that the difference between the two acquisition criteria is reduced when the value of CT_p increases. The impact of the C/N$_0$ and T_p on the two figures of merit is represented in Figure 13.

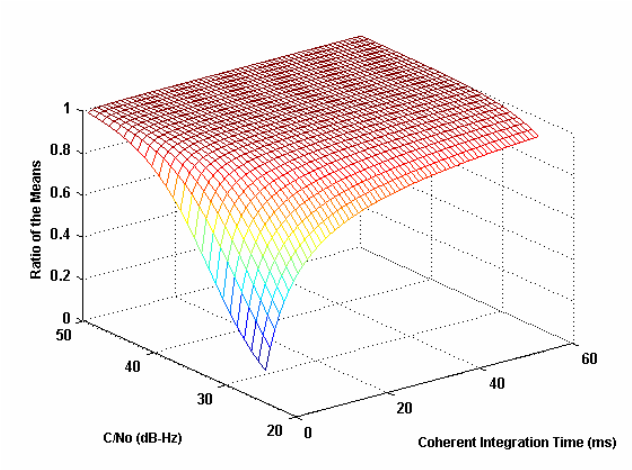

Figure 13 – Impact of the Coherent Integration Time and the C/N$_0$ on $FOM1$ and $FOM2$

Knowing that the difference between two independent random variables has a distribution which is the convolution between the first variable distribution and the opposite of the second variable distribution [Papoulis, 1991], it can be written that:

$$p_{T_{new}}(x) = p_{T_{BOC}}(x) * p_{T_{BOC/PRN}}(-x) \qquad (28)$$

where p_α is the distribution of the random variable α.

As a consequence, it is possible to model through simulations the distribution of T_{new} as a non-central Chi-square distribution. Therefore, the probability of detection of the main peak using the new acquisition criteria can be estimated. Making the same assumptions as in the first section, Figure 14 and Figure 15 are obtained.

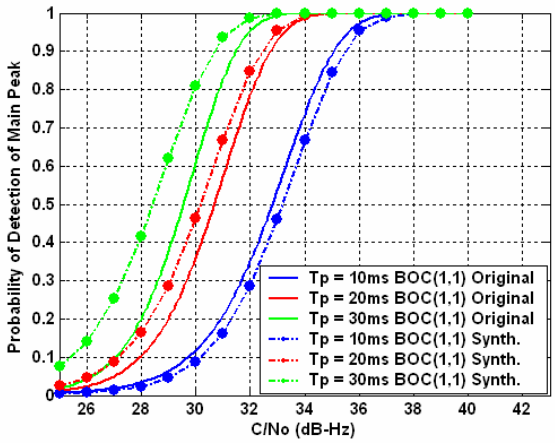

Figure 14 – Probability of Detection of the Main Peak using the Standard BOC(1,1) and the New Acquisition Criteria with no Non-Coherent Summations and Coherent Integration Times of 10, 20 and 30 ms.

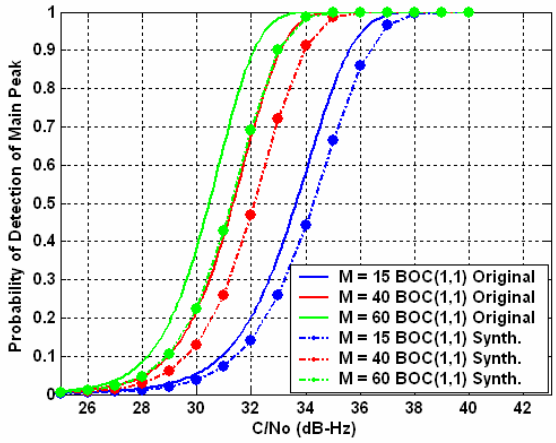

Figure 15 - Probability of Detection of the Main Peak using the Standard BOC(1,1) and the New Acquisition Criteria with 15, 40 and 60 Non-Coherent Summations and a Coherent Integration Time of 1 ms.

As expected, the coherent integration time has a greater effect on the acquisition performance than the non-coherent summation number compared to the original BOC(1,1) acquisition strategy. For long coherent integrations, the new method even outperforms the standard BOC(1,1) method. This is very important as the GALILEO L1 civil signal will have a pilot data channel authorizing longer coherent integrations (however long coherent integrations raise problems for the Doppler bin size). This might appear confusing as the two figures of merit studied previously showed that, for any coherent integration time, the standard method would do better than the new technique. However, when considering acquisition, this phenomenon will also impact the acquisition threshold determination in the same way, compensating for the first effect. Concerning the use of non-coherent summations, as expected, its value does not have a great impact on the difference between the two methods. However, it can be seen that in all the simulated cases the maximum loss using the new method compared to the original one is smaller than 1 dB. As a consequence, the use of the new synthesized correlation function for acquisition purposes seems very relevant in terms of performance. However, it also has two main drawbacks. The first one is the use of four correlators for each acquisition bin instead of two in the standard case. The second one is that the maximum code delay bin width is limited by the width of the synthesized correlation function. This could imply an increase in the number of bins to search during acquisition compared to methods using non-coherently the side-lobes of the BOC(1,1) spectrum (Martin et al., 2003).

CONCLUSIONS

A new unambiguous BOC(1,1) tracking method has been proposed, based on correlations with the local

BOC(1,1) signal and the local PRN code without the sub-carrier. This method can be directly extended to any BOC(n,n) signals as they have the exact same correlation properties.
The use of the new tracking algorithm fully cancels any bias threat, offering reliable measurements without the need for checking that lock is on the correct peak. Many performance aspects of the proposed technique were analyzed: acquisition normalized DLL discriminator tracking error, multipath error envelope. In each case, the new algorithm showed performances that were either better than in the standard case, or very slightly worse (< 1 dB for tracking in terms of C/N_0). These features make the new tracking algorithm extremely interesting for future GALILEO L1 civil receivers as it ensures reliable measurements while maintaining an extremely good tracking performance.

ACKNOWLEDGMENT
The authors would like to thank the France-Canada Research Fund for its financial support.

REFERENCES
Bastide, F., O. Julien, C. Macabiau, and B. Roturier (2002), *Analysis of L5/E5 Acquisition, Tracking and Data Demodulation Thresholds*, Proceedings of U.S. Institute of Navigation GPS (Portland, OR, USA, Sept. 24-27), pp. 2196-2207.

Betz, J.W. (2002), *Binary Offset Carrier Modulations for Radionavigation*, Navigation, Journal of the Institute of Navigation, Winter 2001-2002, Vol. 48, Number 4, pp. 227-246.

Fine, P., and W. Wilson (1999), Tracking Algorithm for GPS Offset Carrier Signals, Proceedings of U.S. Institute of Navigation NTM (San Diego, CA, USA, Jan. 25-27), pp. 671-676.

Gibbon, G (2004), *Welcome Progress in GNSS Talks*, GPS World, February issue.

Godet, J., J.C. de Mateo, P. Erhard, and O. Nouvel (2002), *Assessing the Radio Frequency Compatibility between GPS and Galileo*, Proceedings of U.S. Institute of Navigation GPS (Portland, OR, USA, Sept. 24-27), pp. 1260-1269.

Lin, V.S, P.A. Dafesh, A. Wu, and C.R. Cahn (2003), *Study of the Impact of False Lock Points on Subcarrier Modulated Ranging Signals and Recommended Mitigation Approaches*, Proceedings of U.S. Institute of Navigation AM (Albuquerque, NM, USA, June 23-25), pp. 156-165.

Martin, N., V. Leblond, G. Guillotel, and V. Heiries (2003), *BOC(x,y) Signal Acquisition Techniques and Performances*, Proceedings of U.S. Institute of Navigation GPS/GNSS (Portland, OR, USA, Sept. 9-12), pp. 188-198.

Papoulis, A. (1991), *Probability, Random Variables and Stochastic Processes*, Third Edition, McGraw Hill International Editions.

Ward, P. (2004), *A Design Technique to Remove the Correlation Ambiguity in Binary Offset Carrier (BOC) Spread Spectrum Signals (Revised Version)*, Proceedings of U.S. Institute of Navigation NTM (San Diego, CA, USA, Jan. 26-28), pp. 886-896.

APPENDIX A: NOISE CORRELATION BETWEEN BOC(1,1)/BOC(1,1) AND BOC(1,1)/PRN CHANNELS
Note: unlike the main part of the article, the time in this appendix will now be in seconds and not in chips.

The random variables involved in T_{BOC} are n_{IBOC} and n_{QBOC}. The random variables involved in T_{BOC} are $n_{IBOC,PRN}$ and $n_{QBOC,PRN}$. These random variables are defined as:

$$n_{IBOC} = \frac{1}{M}\sum_{k=1}^{M}\begin{pmatrix} n(k)\times\cos\left(2\pi F_I kT_s - \hat{\theta}\right) \\ \times sc(kT_s - \hat{\tau})\times c\left(kT_s - \hat{\tau}\right)\end{pmatrix}$$

$$n_{QBOC} = \frac{1}{M}\sum_{k=1}^{M}\begin{pmatrix} n(k)\times\sin\left(2\pi F_I kT_s - \hat{\theta}\right) \\ \times sc(kT_s - \hat{\tau})\times c\left(kT_s - \hat{\tau}\right)\end{pmatrix}$$

$$n_{IBOC,PRN} = \frac{1}{M}\sum_{k=1}^{M} n(k)\times\cos\left(2\pi F_I kT_s - \hat{\theta}\right)\times c(kT_s - \hat{\tau})$$

$$n_{IBOC,PRN} = \frac{1}{M}\sum_{k=1}^{M} n(k)\times\sin\left(2\pi F_I kT_s - \hat{\theta}\right)\times c(kT_s - \hat{\tau})$$

where sc is the sub-carrier function, F_I is the signal intermediate frequency, $\hat{\theta}$ and $\hat{\tau}$ are the phase and code estimates, and T_s is the sampling period.

It is known that n_{IBOC} and n_{QBOC} are not correlated. So the correlation between n_{IBOC} and $n_{IBOC,PRN}$ or $n_{QBOC,PRN}$ just needs to be determined. In order to do this, the correlation function $R_{IBOC,IBOC/PRN}(\tau)$ between n_{IBOC} and $n_{IBOC,PRN}$ has to be computed. Without loss of generality, this correlation function will be determined with the equivalent continuous time signals.
The Integrate and Dump filter can be seen as a low-pass filter that has an impulse response denoted as

$$f(t) = \frac{1}{T_p}\,\mathrm{rect}_{\frac{T_p}{2}}\left(\frac{t}{T_p}\right)$$

where $rect_\alpha\left(\frac{x}{y}\right)$ is the value in x of a rectangle that is centred in α and whose length is y.

So,

$n_{IBOC}(nT_p) = (f * s_{IBOC})(nT_p)$, and

$n_{IBOC/PRN}(nT_p) = (f * s_{IBOC/PRN})(nT_p)$

where

$s_{IBOC}(t) = n(t) \times \cos\left(2\pi F_I t - \hat{\theta}\right) \times sc(t-\hat{\tau}) \times c(t-\hat{\tau})$

, and

$s_{IBOC/PRN}(t) = n(t) \times \cos\left(2\pi F_I t - \hat{\theta}\right) \times c(t-\hat{\tau})$

As these two signals are passing through the same filter, the correlation function of the integrated signals can be expressed as:

$R_{IBOC,IBOC-PRN}(\tau) = f(\tau) * f(-\tau) * R_{s_{IBOC},s_{IBOC/PRN}}(\tau)$

where $R_{s_{IBOC},s_{IBOC-PRN}}(\tau)$ is the correlation between $s_{IBOC}(t)$ and $s_{IBOC,PRN}(t)$.

It can then easily be seen that:

$$R_{s_{IBOC},s_{IBOC/PRN}}(\tau) = E\begin{bmatrix} n(t) \times \cos\left(2\pi F_I t - \hat{\theta}\right) \times sc(t-\hat{\tau}) \times c(t-\hat{\tau}) \\ \times n(t-\tau) \times \cos\left(2\pi F_I (t-\tau) - \hat{\theta}\right) \times c(t-\tau-\hat{\tau}) \end{bmatrix}$$

Using the classical orthogonal decomposition of narrow bandwidth noise, we can write

$n(t) = X(t)\cos\left(2\pi F_I t - \hat{\theta}\right) - Y(t)\sin\left(2\pi F_I t - \hat{\theta}\right)$

As the doubled frequency terms are further eliminated by the integration:

$$R_{s_{IBOC},s_{IBOC/PRN}}(\tau) = \frac{1}{4}E\begin{bmatrix} X(t) \times sc(t-\hat{\tau}) \times c(t-\hat{\tau}) \\ \times X(t-\tau) \times c(t-\tau-\hat{\tau}) \end{bmatrix}$$

As the noise is independent from the PRN code and BOC sub-carrier, it can be written:

$$R_{s_{IBOC},s_{IBOC/PRN}}(\tau) = \frac{1}{4}R_X(\tau)E\begin{bmatrix} sc(t-\hat{\tau}) \times c(t-\hat{\tau}) \\ \times c(t-\tau-\hat{\tau}) \end{bmatrix}$$

The code signal can be expressed as:

$$c(t) = \sum_{k=-\infty}^{+\infty} c(k) rect_{kT_c}\left(\frac{t}{T_c}\right)$$

where $c(k)$ is the (-1;+1) digital sequence and T_c is the chip length.

Therefore,

$$E\left[sc(t-\hat{\tau}) \times c(t-\hat{\tau}) \times c(t-\tau-\hat{\tau})\right] = E\begin{bmatrix} \sum_{k=-\infty}^{+\infty} c(k) sc(t-\hat{\tau}) rect_{\hat{\tau}+kT_c}\left(\frac{t}{T_c}\right) \\ \times \sum_{k=-\infty}^{+\infty} c(k) rect_{\tau+\hat{\tau}+kT_c}\left(\frac{t}{T_c}\right) \end{bmatrix}$$

In that case, this cross-correlation can be expressed as:

$$E\left[sc(t-\hat{\tau}) \times c(t-\hat{\tau}) \times c(t-\tau-\hat{\tau})\right] = \frac{1}{T_c}\sum_{m=-\infty}^{+\infty} R_c(m) R_{sboc-rect,rect}(\tau - mT_c)$$

Assuming the code is an independent sequence of bits, we have then

$$E\left[sc(t-\hat{\tau}) \times c(t-\hat{\tau}) \times c(t-\tau-\hat{\tau})\right] = \frac{1}{T_c}R_{sboc-rect,rect}(\tau)$$

In order to finish the calculation, $R_{sboc-rect,rect}(\tau)$ has to be determined:

$$R_{sboc-rect,rect}(\tau) = \int_0^{T_c} sc(t) \times rect_0\left(\frac{t}{T_c}\right) \times rect_\tau\left(\frac{t}{T_c}\right) dt$$

,and

$sc(t) = rect_{\frac{T_c}{4}}\left(\frac{t}{\frac{T_c}{2}}\right) - rect_{\frac{3T_c}{4}}\left(\frac{t}{\frac{T_c}{2}}\right)$ for a sine phasing of the BOC(1,1) sub carrier. So it can be shown that this correlation function can be expressed as:

$$R_{sboc-rect,rect}(\tau) = \frac{T_c}{2}\left(tri_{-\frac{T_c}{2}}\left(\frac{\tau}{T_c}\right) - tri_{\frac{T_c}{2}}\left(\frac{\tau}{T_c}\right)\right)$$

which is equal to equation (6).

Therefore:

$$R_{s_{IBOC},s_{IBOC-PRN}}(\tau) = \frac{1}{8}R_X(\tau) \times \left[tri_{-\frac{T_c}{2}}\left(\frac{\tau}{T_c}\right) - tri_{\frac{T_c}{2}}\left(\frac{\tau}{T_c}\right)\right]$$

,and $R_X(\tau) = h(\tau) * h(-\tau) * \frac{N_0}{2}\delta(\tau)$

So:

$R_{IBOC,IBOC-PRN}(\tau) = f(\tau) * f(-\tau) * R_{s_{IBOC},s_{IBOC-PRN}}(\tau)$

In order to determine the correlation between the noise samples in the acquisition process, we need to determine $R_{IBOC,IBOC-PRN}(0)$.

As $R_{sboc-rect,rect}(0) = 0$, then $R_{IBOC,IBOC-PRN}(0) = 0$.

As a consequence, the correlation between the two correlators' noise considered is null when no front-end filter is considered.